Dr. Saprizal Turnitin Lampiran C8

by Saprizal Hadisaputra

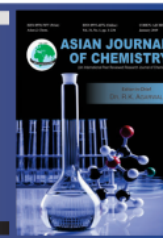
ab initio Study of Corrosion Inhibition Performance of Dibenzo-diaza-15-crown-5 and its Heterocyclic Analogs

S. Hamdiani[1], I.H. Rohimah[1], N. Nuryono[2], A.A. Purwoko[3], L.R.T. Savalas[3] and S. Hadisaputra[3,*]

[1]Department of Chemistry, Faculty of Mathematics and Natural Science, University of Mataram, Mataram 83125, Indonesia
[2]Department of Chemistry, Universitas Gadjah Mada, Sekip Utara, Yogyakarta 55281, Indonesia
[3]Chemistry Education Division, Faculty of Teacher Training and Science Education, University of Mataram, Lombok 83125, Indonesia

*Corresponding author: E-mail: rizal@unram.ac.id

The corrosion inhibition efficiency of dibenzo-diaza-15-crown-5 (N) and its heterocyclic analogs containing O, S, and P atoms were investigated by *ab initio* MP2 calculations in aqueous phase. Heteroatoms have a significant role in the corrosion inhibition performance of the studied systems. The geometry parameter shows that the decrease of bond length corresponds to the increase of heteroatom covalent radius. It was revealed that phosphorus more easily donates its electrons to iron than other heteroatoms. Quantum parameters such as high occupied molecular orbital energies (E_{HOMO}) and the fraction of electrons transferred (ΔN) have a linear relationship with inhibition efficiencies (IE %). Analysis of second order interaction energies showed the highest back-donation contribution of metal to phosphorus. Theoretical calculations shows that corrosion inhibition increases in the sequence of oxygen < nitrogen < sulfur < phosphorus.

Keywords: Crown ether, Corrosion inhibition, Heteroatom, MP2 calculation.

INTRODUCTION

Corrosion is a process that destroys the structure of less noble metals and alloys and that causes high economic losses if not prevented [1]. One method of corrosion prevention is to apply organic inhibitors to metal surfaces [2-9]. The main advantages of organic inhibitors are that they are environmentally friendly and highly efficient. The most efficient organic inhibitors have electronegative functional groups such as oxygen, nitrogen, sulfur, phosphorus and π-electrons in their molecular frameworks [10,11]. These functional and π-electron groups facilitate interaction between organic inhibitors and metal surfaces *via* a coordinate covalent bond (chemical adsorption) or an electrostatic interaction (physical adsorption) [12]. The formation of a complex between the molecular inhibitor and the metal creates a uniform thin film layer on the metal surface thus preventing contact between metal and corrosive medium [13].

Major research efforts have been devoted to several organic inhibitors [14-19]. However, only a few studies have been conducted to investigate the role of crown ethers as organic corrosion inhi-bitors. The properties of crown ethers can be easily modified by adding heteroatoms (O, N, S, and P), and

adding a π-electron in multiple bonds, in order to meet the criteria for efficient corrosion inhibition. Furthermore, crown ethers are environ-mentally friendly and non-toxic, making them suitable as green corrosion inhibitors.

Quantum mechanical theoretical studies have examined extensively the interaction of crown ethers with some metals. Such studies have included the effect of macrocyclic ring size, heteroatoms, electron donating and withdrawing substitution in the metal ion/crown ether interaction [20-23]. The quantum chemical approach has also been used to investigate the corrosion inhibition characteristics of many organic inhibitors [24-29]. In this paper, the influence of heteroatom types on the corrosion inhibitor performance of dibenzo-diaza-15-crown-5 and its heterocyclic analogs is investigated.

COMPUTATIONAL METHODS

The geometries of crown ether were determined by second order Møller-Plesset perturbation theory. For reducing of computational effort, single iron cluster (the simplest possible form of a cluster) was selected. This study used the LANL2DZ basis set with effective core potential, including 10 electrons

in the core for iron and leaving 16 valence electrons. For the crown ether atom, the 6-31G(d) basis set was used. The solvent effects were included using the polarized continuum model (PCM) as implemented in the Gaussian code, because corrosion dominantly occurred in an aqueous environment. The dielectric constant for the water solvent was taken as 78.4. In employing the PCM model, structure re-optimization in the presence of solvent was found to have a minor influence on energetic levels, and therefore single-point calculations on gas-phase geometries are sufficient for such measurements [20,21,23,29]. All calculations, including the quantum chemical parameters, were performed using the Gaussian 03 package [30]. The quantum chemical parameters, such as energy of the highest occupied molecular orbital (E_{HOMO}), energy of the lowest unoccupied molecular orbital (E_{LUMO}), ionization potential (I), electron affinity (A), absolute electronegativity (χ), hardness (η), softness (σ), fraction of electrons transferred (ΔN), total energy charge (E_T) and corrosion inhibitor (IE %) efficiencies were calculated from previously reported equations [22-24].

RESULTS AND DISCUSSION

Dibenzo-diaza-15-crown-5 (N) and its heterocyclic analogs containing O, S, P heteroatoms were investigated as depicted in **Scheme-I**. Fig. 1 shows the structure of optimized geometries of dibenzo-diaza-15-crown-5 and its heterocyclic analogs containing O, S, and P heteroatoms calculated by MP2/6-31G(d) level of theory. The structure optimization was conducted by Cs conformational selection. The studied compounds are planar and show no significant structural changes due to the addition of heteroatoms. The presence of benzene ring makes molecule rigid and leads to a small number of conformational isomers; as a result, the computational effort was also reduced.

Table-1 shows selected geometrical parameters of inhibitor interactions with Fe in aqueous phases. The bond length between heteroatoms and Fe follows the sequence of Fe-P, Fe-S, Fe-N, and Fe-O, being 2.422, 2.404, 2.011 and 1.976 Å, respectively. The bond-length of studied molecule is aligned with the covalent radius of two interacting atoms (covalent radius is 1.07, 1.05, 0.71, 0.66 and 1.32 Å for P, S, N, O, and Fe, respectively) [31]. The size of covalent radius means that heteroatoms such as P and S more easily donate their electrons to Fe, whereas O has
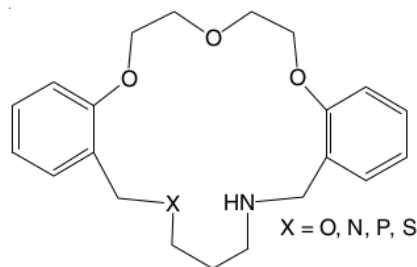
Scheme-I: Molecular structure of the dibenzo-diaza-15-crown-5 (N)

the opposite behaviour due to its outer electrons being more closely held around the radius. Hence, heteroatoms P and S are predicted to contribute more to increasing the efficiency of corrosion inhibitors.

The effectiveness of corrosion inhibitors depends not only on spatial molecular structures but also on the nature of molecular electronic structures. The high occupied molecular orbital (HOMO) and low unoccupied molecular orbital (LUMO) energies related to the reactivity of dibenzo-diaza-15-crown-5 ether and its heterocyclic analogs are reported in Table-2. The interaction between E_{HOMO} and E_{LUMO} of reacting species lead to the transition of electrons within molecules [32].

The transition of electrons, including donation and acceptance, are measured by the energy value of molecular orbitals. The HOMO energy indicates the tendency of molecules towards the donation of electrons. It is found that crown ethers with P and S heteroatoms have higher HOMO energies than those with O and N heteroatoms. Therefore, they are more intent on donating electrons than crown ethers with O and N heteroatoms. This trend can be used as a preliminary prediction that dibenzo-15-crown-5 with P and S heteroatoms will have higher corrosion inhibition efficiency.

Another important parameter for evaluating the efficiency of corrosion inhibitors is the value of separation energy, ΔE ($E_{LUMO} - E_{HOMO}$). The smaller ΔE value, the more reactive the inhibitor molecules are and more easily they are adsorbed onto the metal surface. Table-2 shows that crown ether containing P heteroatom has the smallest ΔE and the largest E_{HOMO}. It is predicted that adding a P heteroatom to inhibitor framework will lead to the maximum corrosion inhibition efficiency.

TABLE-1
SELECTED GEOMETRICAL PARAMETERS OF Fe-DIBENZO-DIAZA-15-CROWN-5 (N)
AND ITS HETEROCYCLIC ANALOGS IN AQUEOUS PHASE

| Oxygen (O)		Nitrogen (N)		Phosphor (P)		Sulfur (S)	
Bond	Bond length (Å)	Bond	Bond length (Å)	Bond	Bond length (Å)	Bond	Bond length (Å)
C10-C11	1.522	C10-C11	1.514	C10-C11	1.459	C10-C11	1.466
C10-Fe52	1.897	C10-Fe54	1.909	C10-Fe53	2.090	C10-Fe52	2.106
C11-Fe52	2.007	C11-Fe54	2.005	C11-Fe53	2.009	C11-Fe52	1.982
C12-Fe52	2.555	C12-Fe54	2.529	C12-Fe53	2.825	C12-Fe52	2.763
C17-Fe52	2.687	C17-Fe54	2.687	C17-Fe53	2.208	C17-Fe52	2.208
O20-Fe52	2.926	O20-Fe54	2.822	O20-Fe53	2.822	O20-Fe52	2.822
Fe52-O54	1.976	Fe54- N54	2.011	Fe53-P54	2.422	Fe52-S54	2.404
Angle (Å)	Bond angle (Å)	Angle (Å)	Bond angle (Å)	Angle (Å)	Bond angle (Å)	Angle (Å)	Bond angle (Å)
C10-Fe52-O54	98.441	C10-Fe54-N21	88.041	C10-Fe53-P21	91.809	C10-Fe52-S21	95.105
C11-Fe52-O54	72.726	C11-Fe54-N21	72.833	C11-Fe53-P21	74.559	C11-Fe52-S21	76.747
O20-C10-Fe52	120.823	O20-C10-Fe54	114.147	O20-C10-Fe53	130.246	O20-C10-Fe52	131.88
C10-Fe52-C11	45.802	C10-Fe54-C11	45.435	C10-Fe53-C11	41.640	C10-Fe52-C11	41.8930
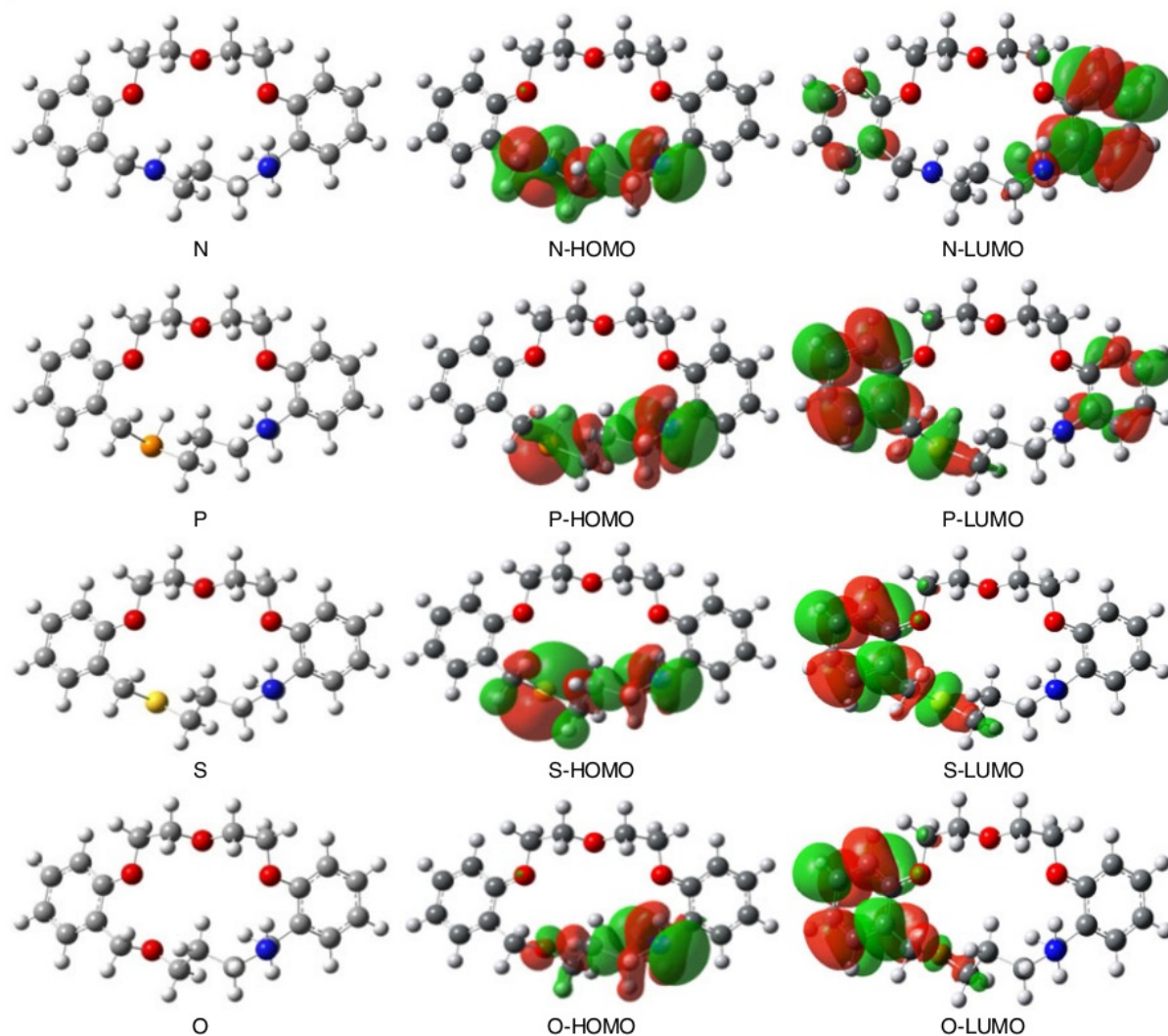
Fig. 1. Optimized structures and HOMO and LUMO orbitals of the studied free molecules, determined using MP2/6-31G(d) level of theory

TABLE-2
QUANTUM CHEMICAL PARAMETERS FOR DIBENZO-DIAZA-15-CROWN-5 (N) AND ITS HETEROCYCLIC
ANALOGS IN AQUEOUS PHASES, DETERMINED USING MP2/6-31G(d) LEVEL OF THEORY

	E_{HOMO} (eV)	E_{LUMO} (eV)	ΔE (eV)	I (eV)	A (eV)	χ (eV)	η (eV)	σ (eV)	ΔN	E_T
N	-8.4094	3.7619	12.1713	8.4094	-3.7619	2.3237	6.0856	0.1643	0.3842	-1.5214
P	-8.2401	3.6577	11.8979	8.2401	-3.6577	2.2912	5.9489	0.1681	0.3957	-1.4872
S	-8.3846	3.5265	11.9112	8.3846	-3.5260	2.4290	5.9556	0.1679	0.3837	-1.4889
O	-8.4344	3.7519	12.1864	8.4344	-3.7519	2.3413	6.0932	0.1641	0.3823	-1.5232

Hard-soft-acid-base (HSAB) properties can be used to predict the bonding tendencies between inhibitors and metal atoms. On the other hand, frontier molecular orbital controls interaction concepts [32]. In general, HSAB rule is that hard acids are prone to interact with hard bases and soft acids prefer to interact with soft bases. Metal atoms are known to be soft bases and so soft base inhibitors are more effective for interacting with metal atoms. Large HOMO-LUMO energy gap is a characteristic of hard molecules, whereas small HOMO-LUMO energy gap is a characteristic of soft molecules. The molecules with the smallest energy gap (ΔE) and the greatest softness (σ) value have the highest inhibitor efficiency. From Table-2, it can be observed that P heteroatom has the highest σ value, and the sequence of soft properties as well as reactivity is O < N < S < P. Table-2 also shows the value of hardness (η) properties of the inhibitors. The value of hardness properties is inversely proportional to the nature of softness. This shows that molecule with the lowest global hardness (the highest value of global softness) is the best inhibitor and *vice-versa*.

The number of electrons transferred (ΔN) is also depicted in Table-2. Based on Lukovits's study [33], if ΔN value < 3.6, the efficiency of the inhibitor will increase due its donating of electrons to the metal surface. The greater the value of ΔN, the greater the ability of inhibitor to donate electrons to the metal surface. This shows that P heteroatom has the highest fraction of electrons transferred, and this is associated with the highest inhibitor efficiency, whereas O has the least fraction and this is associated with the least inhibitor efficiency. Table-2 also shows the total energy charge (E_T) value of < 0. This indicates that transfer of charge occurring from the inhibitor to metal atom will be followed by back donations. However, it needs to be

Fe-N   Fe-N HOMO   Fe-N LUMO

Fe-P   Fe-P HOMO   Fe-P LUMO

Fe-S   Fe-S HOMO   Fe-S LUMO
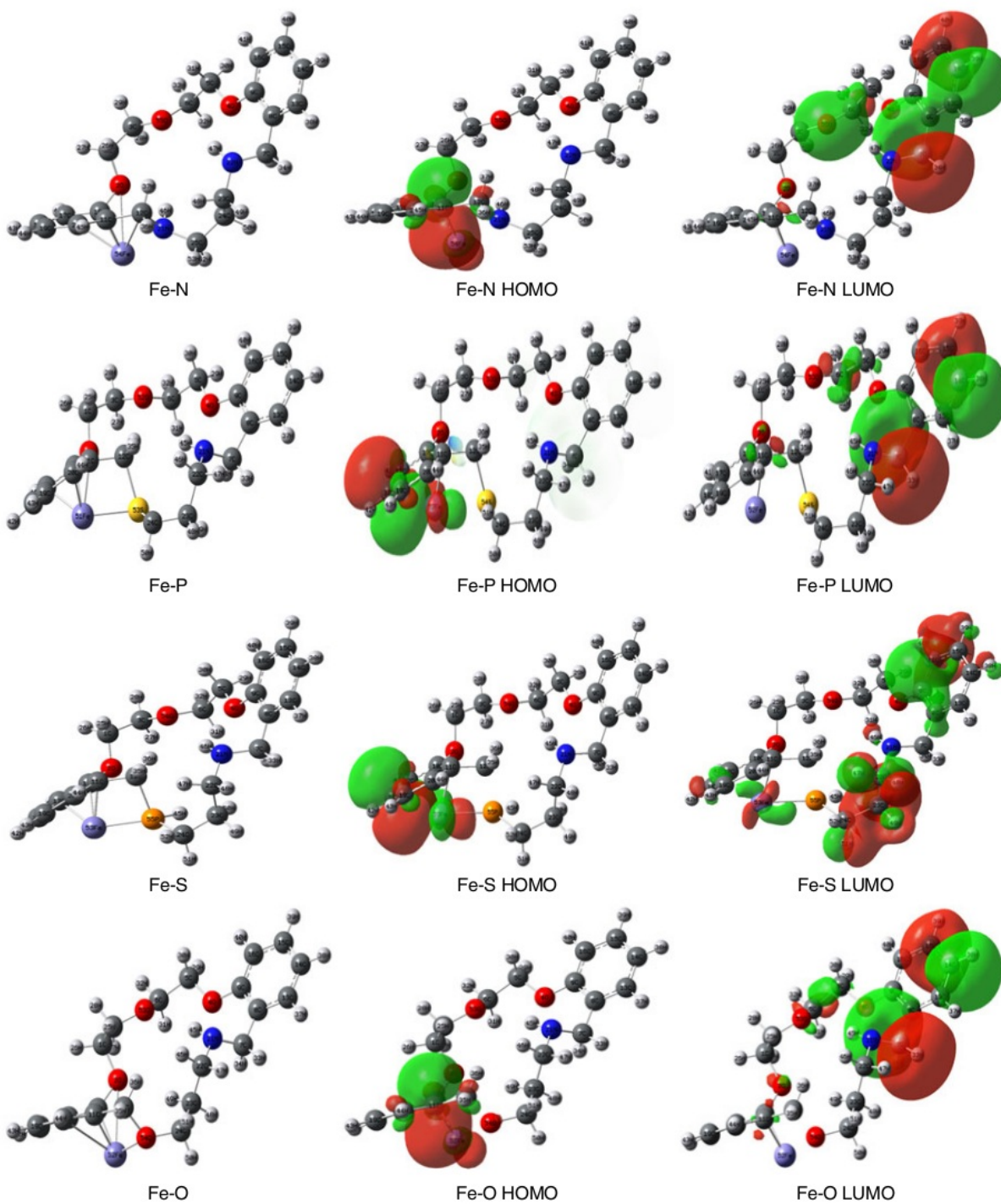
Fe-O   Fe-O HOMO   Fe-O LUMO

Fig. 2. Optimized structures and HOMO and LUMO orbitals of the studied Fe-inhibitors, determined using MP2/6-31G(d) LANL2DZ ECP and 6-31G(d) level of theory

noted that the E_T value cannot be used to predict that back-donation is going to occur; $E_T < 0$ is only established if both processes occur. The calculation of total energy charge shows that P heteroatom has the largest E_T value, so it is predicted that P has the highest corrosion inhibitor efficiency. This trend is linear, with the value of back-donation from examining the value of the second order interaction energy presented in Table-3.

Figs. 1 and 2 show the frontier molecular orbital visualization of dibenzo-diaza-15-crown-15 and its heterocyclic analogs and Fe-inhibitors calculated by LANL2DZ ECP and 6-31G(d) levels of theory. They indicate that HOMO of these crown ether compounds matches with the heteroatom in which the electron density accumulates on the heteroatom site. As expected, the heteroatoms have a significant contribution to interaction with metal surfaces. The correlation between the E_{HOMO}, electron transferred and binding energy with inhibition efficiencies is depicted in Fig. 3. A linear correlation has been identified between E_{HOMO} and inhibition efficiency, electrons transferred and inhibition efficiency of $r^2 = 0.9985$ and 0.9726, respectively.

In order to investigate the correlation of the quantum chemical parameters with corrosion inhibitor performance, the calculated inhibition efficiencies for the studied system have been determined using the formula previously reported by Obayes *et al.* [34]. The calculated inhibition efficiency values are depicted in Table-3. The results show that the presence of

O, N, S, and P heteroatoms on the framework of dibenzo crown ether increases inhibition efficiency in the following sequence O < N < S < P. The same trend has also been reported by other researchers [8]. The addition of a single P atom to the framework of crown ether led to an increase in the corrosion inhibition efficiency of 1.97 % and the addition of single O atoms led to a 0.19 % decrease in corrosion inhibition efficiency. These results are positively correlated with an increase in the energy E2 values of interactions between Fe and inhibitors. Furthermore, the second order interaction energies indicate that back-donation has a significant role in the studied systems. Selected maximum back-donation from NBO calculations shows that the P heteroatom has the highest value, of 14.77 kcal mol^{-1}, followed by S, O, and N, at 5.91, 1.52, and 1.01 kcal mol^{-1}, respectively. These trends are in accordance with the quantum parameters as well as with the efficiency of corrosion inhibitors of dibenzo-diaza-15-crown-5 and its heterocyclic analogs.

Conclusion

An *ab initio* MP2 method has been used to calculate the efficiency of corrosion inhibition of the dibenzo-diaza-15-crown-5 (N) and its heterocyclic analogs containing O, S and P atoms. Quantum parameters such as the highest occupied molecular orbital E_{HOMO}, the lowest unoccupied molecular
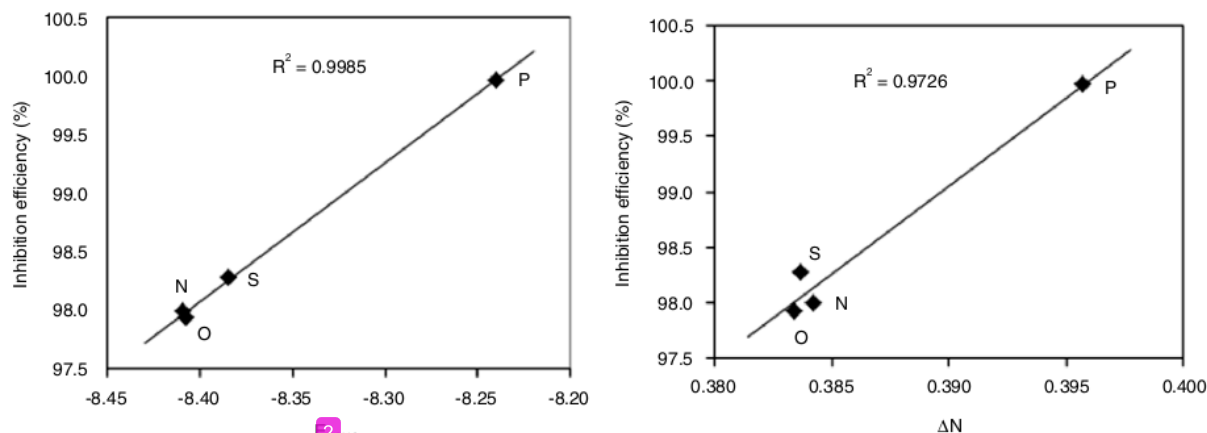

Fig. 3. Correlation between E_{HOMO}, the number of electrons transferred ΔN and corrosion inhibition efficiency IE % of the studied systems

TABLE-3
SELECTED VALUES OF THE MAXIMUM SECOND-ORDER INTERACTION ENERGIES (E2), THE MAXIMUM BACK-DONATING
INTERACTION ENERGIES (E*2), BINDING ENERGIES (ΔE_b) AND THE CORROSION INHIBITION EFFICIENCY (IE, %)

	Maximum donation NBO		Maxi-E2 (kcal mol^{-1})	Back donation NBO		Maxi-E*2 (kcal mol^{-1})	ΔE_b (kcal mol^{-1})	IE (%)
	Donor	Acceptor		Donor	Acceptor			
Fe-N	LP(1)N21	LP*(3)Fe54	65.95					
	LP(1)N21	RY*(4)Fe54	1.95	LP*(4)Fe54	RY*(1)N21	1.01	-304.55	98.00
	LP(1)N21	RY*(3)Fe54	3.18					
Fe-P	LP(1)P55	LP*(4)Fe53	53.38					
	LP(1)P55	RY*(4)Fe53	4.80	LP*(4)Fe53	RY*(1)P5	14.77	-330.41	99.97
	LP(1)P55	RY*(4)Fe53	5.56					
Fe-S	LP(2)S54	LP*(4)Fe52	40.59					
	LP(1)S54	RY*(4)Fe52	2.48	LP*(4)Fe52	RY*(1)S54	5.91	-304.21	98.28
	LP(1)S54	RY*(3)Fe52	5.43					
Fe-O	LP(2)O54	LP*(4)Fe52	51.12					
	LP(1)O54	LP*(4)Fe52	3.05	LP*(3)Fe52	RY*(1)O54	1.52	-297.07	97.71
	LP(2)O54	RY*(3)Fe52	2.02					

orbitals E_{LUMO}, ionization potential, electron affinity, absolute electronegativity, hardness, softness, fraction of electron transferred, total energy charge are used to explain the phenomena of corrosion efficiency inhibitors. For the systems under consideration, the calculation results indicate that quantum parameters have a linear correlation with corrosion inhibition efficiency. The calculated corrosion inhibition efficiency of crown ether is in accordance with the calculation of binding energy and second order interaction energy. The highest corrosion inhibitor efficiency is generated by P heteroatom and the lowest by O heteroatom. Furthermore, it is found that back-donation contributes further to binding, resulting in P heteroatoms having the highest efficiency in terms of corrosion inhibition.

ACKNOWLEDGEMENTS

CONFLICT OF INTEREST

The authors declare that there is no conflict of interests regarding the publication of this article.

REFERENCES

1. H.H, Uhlig and R.W. Revie, Corrosion and Corrosion Control, John Wiley & Sons, New York: USA (1985).
2. Y. Qiang, S. Zhang, L. Guo, S. Xu, L. Feng, I.B. Obot and S. Chen, *J. Clean. Prod.*, **152**, 17 (2017); https://doi.org/10.1016/j.jclepro.2017.03.104.
3. M. Mobin and M. Rizvi, *Carbohydr. Polym.*, **160**, 172 (2017); https://doi.org/10.1016/j.carbpol.2016.12.056.
4. T. Douadi, H. Hamani, D. Daoud, M. Al-Noaimi and S. Chafaa, *J. Taiwan Inst. Chem. Eng.*, **71**, 388 (2017); https://doi.org/10.1016/j.jtice.2016.11.026.
5. J. Bhawsar, P. Jain, M.G. Valladares-Cisneros, C. Cuevas-Arteaga and M. Rani, *Int. J. Electrochem. Sci.*, **133**, 200 (2018).
6. P.B. Raja, M. Ismail, S. Ghoreishiamiri, J. Mirza, M.C. Ismail, S. Kakooei and A.A. Rahim, *Chem. Eng. Commun.*, **203**, 1145 (2016); https://doi.org/10.1080/00986445.2016.1172485.
7. G.L.F. Mendonça, S.N. Costa, V.N. Freire, P.N.S. Casciano, A.N. Correia and P. Lima-Neto, *Corros. Sci.*, **115**, 41 (2017); https://doi.org/10.1016/j.corsci.2016.11.012.
8. L. Guo, I.B. Obot, X. Zheng, X. Shen, Y. Qiang, S. Kaya and C. Kaya, *Appl. Surf. Sci.*, **406**, 301 (2017); https://doi.org/10.1016/j.apsusc.2017.02.134.
9. S.K. Shetty and A.N. Shetty, *J. Mol. Liq.*, **225**, 426 (2017); https://doi.org/10.1016/j.molliq.2016.11.037.
10. S. Benabid, T. Douadi, S. Issaadi, C. Penverne and S. Chafaa, *Measurement*, **99**, 53 (2017); https://doi.org/10.1016/j.measurement.2016.12.022.
11. Z. Salarvand, M. Amirnasr, M. Talebian, K. Raeissi and S. Meghdadi, *Corros. Sci.*, **114**, 133 (2017); https://doi.org/10.1016/j.corsci.2016.11.002.
12. Y. Wang and Y. Zuo, *Corros. Sci.*, **118**, 24 (2017); https://doi.org/10.1016/j.corsci.2017.01.008.
13. X. Hou, L. Gao, Z. Cui and J. Yin, *IOP Conf. Series: Earth Environ. Sci.*, **108**, 022037 (2018); https://doi.org/10.1088/1755-1315/108/2/022037.
14. J. Du, Z. Huang, X.Q. Yu and L. Pu, *Chem. Commun.*, **49**, 5399 (2013); https://doi.org/10.1039/c3cc42081g.
15. M. Hong, X. Wang, W. You, Z. Zhuang and Y. Yu, *Chem. Eng. J.*, **313**, 1278 (2017); https://doi.org/10.1016/j.cej.2016.11.030.
16. A.S. Fouda, M. Abdallah, S.M. Al-Ashrey and A.A. Abdel-Fattah, *Desalination*, **250**, 538 (2010); https://doi.org/10.1016/j.desal.2009.02.055.
17. R. Hasanov, S. Bilge, S. Bilgiç, G. Gece and Z. Kiliç, *Corros. Sci.*, **52**, 984 (2010); https://doi.org/10.1016/j.corsci.2009.11.022.
18. H. Lgaz, R. Salghi and I.H. Ali, *Int. J. Electrochem. Sci.*, **13**, 250 (2010).
19. S. Hadisaputra, L.R. Canaval, H.D. Pranowo and R. Armunanto, *Monatsh. Chem.*, **145**, 737 (2014); https://doi.org/10.1007/s00706-013-1129-x.
20. S. Hadisaputra, L.R. Canaval, H.D. Pranowo and R. Armunanto, *Indones. J. Chem.*, **14**, 199 (2014); https://doi.org/10.22146/ijc.21259.
21. L.R. Canaval, S. Hadisaputra and T.S. Hofer, *Phys. Chem. Chem. Phys.*, **17**, 16359 (2015); https://doi.org/10.1039/C5CP01977J.
22. S. Hadisaputra, H.D. Pranowo and R. Armunanto, *Indones. J. Chem.*, **12**, 207 (2012); https://doi.org/10.22146/ijc.21332.
23. S. Hadisaputra, S. Hamdiani, M.A. Kurniawan and N. Nuryono, *Indones. J. Chem.*, **17**, 431 (2017); https://doi.org/10.22146/ijc.26667.
24. A.A. Purwoko and S. Hadisaputra, *Orient. J. Chem.*, **33**, 717 (2017); https://doi.org/10.13005/ojc/330218.
25. S. Kaya, L. Guo, C. Kaya, B. Tüzün, I.B. Obot, R. Touir and N. Islam, *J. Taiwan Inst. Chem. Eng.*, **65**, 522 (2016); https://doi.org/10.1016/j.jtice.2016.05.034.
26. A. Zarrouk, I. El Ouali, M. Bouachrine, B. Hammouti, Y. Ramli, E.M. Essassi, I. Warad, A. Aouniti and R. Salghi, *Res. Chem. Intermed.*, **39**, 1125 (2013); https://doi.org/10.1007/s11164-012-0671-1.
27. I.B. Obot, S. Kaya, C. Kaya and B. Tüzün, *Res. Chem. Intermed.*, **42**, 4963 (2016); https://doi.org/10.1007/s11164-015-2339-0.
28. D. Zhang, Y. Tang, S. Qi, D. Dong, H. Cang and G. Lu, *Corros. Sci.*, **102**, 517 (2016); https://doi.org/10.1016/j.corsci.2015.10.002.
29. S. Saha, A. Hens, N.C. Murmu and P. Banerjee, *J. Mol. Liq.*, **215**, 486 (2016); https://doi.org/10.1016/j.molliq.2016.01.024.
30. M.J. Frisch, G.W. Trucks, H.B. Schlegel, G.E. Scuseria, M.A. Robb, J.R. Cheeseman, J.A. Montgomery, T.J. Vreven, K.N. Kudin, J.C. Burant, J.M. Millam, S.S. Iyengar, J. Tomasi, V. Barone, B. Mennucci, M. Cossi, G. Scalmani, N. Rega, G.A. Petersson, H. Nakatsuji, M. Hada, M. Ehara, K. Toyota, R. Fukuda, J. Hasegawa, M. Ishida, T. Nakajima, Y. Honda, O. Kitao, H. Nakai, M. Klene, X. Li, J.E. Knox, H.P. Hratchian, J.B. Cross, C. Adamo, J. Jaramillo, R. Gomperts, R.E. Stratmann, O. Yazyev, A.J. Austin, R. Cammi, C. Pomelli, J.W. Ochterski, P.Y. Ayala, K. Morokuma, G.A. Voth, P. Salvador, J.J. Dannenberg, V.G. Zakrzewski, S. Dapprich, A.D. Daniels, M.C. Strain, O. Farkas, D.K. Malick, A.D. Rabuck, K. Raghavachari, J.B. Foresman, J.V. Ortiz, Q. Cui, A.G. Baboul, S. Clifford, J. Cioslowski, B.B. Stefanov, G. Liu, A. Liashenko, P. Piskorz, I. Komaromi, R.L. Martin, D.J. Fox, T. Keith, M.A. Al-Laham, C.Y. Peng, A. Nanayakkara, M. Challacombe, P.M.W. Gill, B. Johnson, W. Chen, M.W. Wong, C. Gonzalez and J.A. Pople, Gaussian03, Gaussian, Inc., Pittsburgh, PA, (2003).
31. P. Pyykko and M. Atsumi, *Chem. Eur. J.*, **15**, 186 (2009); https://doi.org/10.1002/chem.200800987.
32. R.G. Pearson, *Inorg. Chem.*, **27**, 734 (1988); https://doi.org/10.1021/ic00277a030.
33. I. Lukovits, E. Kalman and F. Zucchi, *Corrosion*, **57**, 3 (2001); https://doi.org/10.5006/1.3290328.
34. H.R. Obayes, G.H. Alwan, A.H. Alobaidy, M. Al-Amiery, A.A. Kadhum and A.B. Mohamad, *Chem. Cent. J.*, **8**, 21 (2014); https://doi.org/10.1186/1752-153X-8-21.

Dr. Saprizal Turnitin Lampiran C8

1 Saprizal Hadisaputra, Agus Abhi Purwoko, Saprini Hamdiani, N Nuryono. "Which anthocyanin is the best corrosion inhibitor?", IOP Conference Series: Materials Science and Engineering, 2019
Publication

8%

2 Saprizal Hadisaputra, Agus Abhi Purwoko, Rahmawati, Saprini Hamdiani, Yuniar Ponco Prananto, Nuryono. "Theoretical study on the corrosion inhibition performance of dibenzo-18-crown-6 and its derivatives", IOP Conference Series: Materials Science and Engineering, 2019
Publication

6%

3 www.mdpi.com
Internet Source

4%

4 iopscience.iop.org
Internet Source

3%

5 science.uobabylon.edu.iq
Internet Source

2%

6 link.springer.com
Internet Source

1%

7 Bagheri, A.. **"STRUCTURAL STUDY AND INVESTIGATION OF NMR TENSORS IN INTERACTION OF DOPAMINE WITH ADENINE AND GUANINE"**, Bulletin of the Chemical Society of Ethiopia, 2007.
Publication

1%

8 medcraveonline.com
Internet Source

1%

Exclude quotes	Off	Exclude matches	< 1%
Exclude bibliography	On		